

The *Mi-9* Gene from *Solanum arcanum* Conferring Heat-Stable Resistance to Root-Knot Nematodes Is a Homolog of *Mi-1*^{[W][OA]}

Barbara Jablonska², Jetty S.S. Ammiraju³, Kishor K. Bhattarai, Sophie Mantelin, Oscar Martinez de Iarduya⁴, Philip A. Roberts, and Isgouhi Kaloshian*

Department of Nematology, University of California, Riverside, California 92521

Resistance conferred by the *Mi-1* gene from *Solanum peruvianum* is effective and widely used for limiting root-knot nematode (*Meloidogyne* spp.) yield loss in tomato (*Solanum lycopersicum*), but the resistance is ineffective at soil temperatures above 28°C. Previously, we mapped the heat-stable resistance gene *Mi-9* in *Solanum arcanum* accession LA2157 to the short arm of chromosome 6, in a genetic interval as *Mi-1* and the *Cladosporium fulvum* resistance gene *Cf2*. We developed a fine map of the *Mi-9* region by resistance and marker screening of an F₂ population and derived F₃ families from resistant LA2157 × susceptible LA392. *Mi-1* intron 1 flanking primers were designed to amplify intron 1 and fingerprint *Mi-1* homologs. Using these primers, we identified seven *Mi-1* homologs in the mapping parents. *Cf-2* and *Mi-1* homologs were mapped on chromosome 6 using a subset of the F₂. *Cf-2* homologs did not segregate with *Mi-9* resistance, but three *Mi-1* homologs (*RH1*, *RH2*, and *RH4*) from LA2157 and one (*SH1*) from LA392 colocalized to the *Mi-9* region. Reverse transcriptase-polymerase chain reaction analysis indicated that six *Mi-1* homologs are expressed in LA2157 roots. We targeted transcripts of *Mi-1* homologs for degradation with tobacco (*Nicotiana tabacum*) rattle virus (TRV)-based virus-induced gene silencing using *Agrobacterium* infiltration with a TRV-*Mi* construct. In most LA2157 plants infiltrated with the TRV-*Mi* construct, *Mi-9*-mediated heat-stable root-knot nematode resistance was compromised at 32°C, indicating that the heat-stable resistance is mediated by a homolog of *Mi-1*.

Root-knot nematodes (*Meloidogyne* spp.) are root endoparasites of numerous crops worldwide and are the most damaging nematode pest in agriculture (Sasser, 1980). Tomato (*Solanum lycopersicum*, formerly *Lycopersicon esculentum*; Peralta and Spooner, 2005) is a highly susceptible host of several species of root-knot nematodes and incurs yield losses from root-knot infection in warm temperate to tropical regions as well as in greenhouse and other controlled environment production systems. Yield of susceptible tomato cultivars can be reduced by 50% or more in infested

fields (Johnson, 1998). The use of resistant cultivars carrying gene *Mi-1* has proved to be highly effective as a nematode management strategy, and resistant cultivars produce normal yields on infested land (Roberts and May, 1986). As a result, this gene has been exploited extensively in the last two decades for modern tomato cultivar development.

Gene *Mi-1* was introgressed into tomato from its wild relative *Solanum peruvianum* (formerly *Lycopersicon peruvianum*; Peralta and Spooner, 2005) and is the only commercially available source of resistance to root-knot nematodes in this crop. *Mi-1* confers resistance to three species of root-knot nematodes: *Meloidogyne arenaria*, *Meloidogyne incognita*, and *Meloidogyne javanica* (Dropkin, 1969a). In addition to resistance to the three root-knot nematode species, *Mi-1* also confers resistance to certain biotypes of potato aphid (*Macrosiphum euphorbiae*; Rossi et al., 1998; Vos et al., 1998) and two biotypes of the whitefly *Bemisia tabaci* (Nombela et al., 2003). The *Mi-1* gene belongs to the class of resistance (R) genes that contains a coiled-coil, nucleotide-binding site (NBS), and Leu-rich repeats (LRRs; Milligan et al., 1998). Although *Mi-1*-mediated resistance has proven to be highly effective for root-knot nematode control, the resistance is inactive above 28°C soil temperature (Holtzmann, 1965; Dropkin, 1969b). The breakdown of *Mi-1*-mediated resistance due to high temperature has been reported in both greenhouse and field tomato production systems (Philis and Vakis, 1977; Tzortzakakis and Gowen, 1996; Noling, 2000). In fact, temperature sensitivity appears to be a characteristic of several

¹ This work was supported in part by the U.S. Department of Agriculture-National Research Initiative Competitive Grants Program (grant no. 98-35300-6350 to I.K. and P.R.) and by the University of California Agricultural Experiment Station (grants to I.K.).

² Present address: Department of Botany and Plant Sciences, University of California, Riverside, CA 92521.

³ Present address: Arizona Genomics Institute, Department of Plant Sciences, University of Arizona, Tucson, AZ 85725.

⁴ Present address: Fundación AZTI-Tecnalia, Txatxarramendi ugarte, 48395 Sukarrieta, Spain.

* Corresponding author; e-mail isgouhi.kaloshian@ucr.edu; fax 951-827-3719.

The author responsible for distribution of materials integral to the findings presented in this article in accordance with the policy described in the Instructions for Authors (www.plantphysiol.org) is: Isgouhi Kaloshian (isgouhi.kaloshian@ucr.edu).

^[W] The online version of this article contains Web-only data.

^[OA] Open Access articles can be viewed online without a subscription.

www.plantphysiol.org/cgi/doi/10.1104/pp.106.089615

root-knot nematode R genes, having been described in other crop species, including alfalfa (*Medicago sativa*; Griffin, 1969), sweet potato (*Ipomoea batatas*; Jatala and Russell, 1972), and cotton (*Gossypium hirsutum*; Carter, 1982).

Reproduced primarily by outcrossing, *S. peruvianum* is comprised of a genetically heterogeneous group of plants referred to as the *S. peruvianum* complex (Rick, 1979). This wild relative of tomato has proven to be a rich source of disease resistance (Atherton and Rudich, 1986). For example, new sources of root-knot nematode resistance have been identified in accessions of *S. peruvianum* (Ammati et al., 1985, 1986). Inheritance studies of some of these new resistance traits have revealed the presence of additional genes that segregate independently of *Mi-1* (Cap et al., 1993; Veremis and Roberts, 1996b). These genes were distinguished according to resistance phenotype at high temperature or resistance to *Mi-1*-virulent nematode isolates (Veremis and Roberts, 1996a, 1996b). To date, only two of these novel loci have been mapped: the resistance in *S. peruvianum* accession 126443 clone 1MH and in accession LA2157 (Yaghoobi et al., 1995; Veremis et al., 1999). *S. peruvianum* accession 126443 clone 1MH has both heat-stable resistance and resistance to *Mi-1*-virulent root-knot nematodes (Yaghoobi et al., 1995). Both heat-stable resistance and resistance against virulent nematodes are mediated by single dominant genes. It is not clear, however, whether the heat-stable resistance and the resistance to *Mi-1*-virulent nematodes are mediated by the same gene or by tightly linked genes (Yaghoobi et al., 1995; Veremis and Roberts, 1996a).

In LA2157, an accession belonging to the ancient Maranon race complex of *S. peruvianum* from the Maranon drainage area located in northern Peru, the heat-stable root-knot nematode resistance is also mediated by a single dominant gene, *Mi-9* (Veremis et al., 1999). Recently, the Maranon races from northern Peru were reclassified, and accession LA2157 was assigned to a new distinct species, *Solanum arcanum* (Peralta et al., 2005). *Mi-9* confers resistance to *Mi-1*-avirulent isolates of *M. arenaria*, *M. incognita*, and *M. javanica* at 25°C and 32°C but does not confer resistance to *Mi-1*-virulent nematodes (Ammati et al., 1986; Veremis et al., 1999; Veremis and Roberts, 2000). Unlike most *S. arcanum* accessions, LA2157 is self compatible. Using a true F₂ segregating population, *Mi-9* was mapped to chromosome 6 (Veremis et al., 1999). *Mi-9* was further mapped to the short arm of chromosome 6 between markers CT119 and C8B, a similar genetic interval as *Mi-1* (Ammiraju et al., 2003).

Many R genes are members of gene families that seem to be clustered (Michelmore and Meyers, 1998). In these clusters, arrays of paralogs exist that confer resistance to members of distinct groups of pathogens or to multiple variants of a single pathogen (Kesseli et al., 1994; Bendahmane et al., 1999; van der Vossen et al., 2000). Pseudogenes and members with unknown functions also exist within these clusters. Clusters of R genes could be tightly organized or could be

spaced over several megabases (Meyers et al., 1998; Noel et al., 1999). In the *Mi-1* locus on the short arm of tomato chromosome 6, *Mi-1* and six homologs exist in two distinct clusters about 300 kb apart (Vos et al., 1998; Seah et al., 2004). The cluster containing *Mi-1* (also known as *Mi-1.2*) has two additional members, *Mi-1.1* and *Mi-1.3*, and is located near the centromeric proximal end of the chromosome (Kaloshian et al., 1998; Milligan et al., 1998). *Mi-1.3* is a pseudogene, while *Mi-1.1* and *Mi-1* are both transcribed genes with over 91% sequence identity (Milligan et al., 1998). Of these two genes, only *Mi-1* conferred resistance to root-knot nematodes and insects (Milligan et al., 1998; Rossi et al., 1998; Nombela et al., 2003). The short arm of chromosome 6 is characterized by clusters of disease R genes besides *Mi-1* and *Mi-9*. *Cladosporium fulvum* R genes *Cf-2* and *Cf-5* (Dixon et al., 1996, 1998), genes *Ol-4* and *Ol-6* conferring resistance to *Oidium neolycopersici* (Bai et al., 2005), alfalfa mosaic virus R gene, *Am* (Parrella et al., 2004), and possibly *Ty-1* and *Bw-5* conferring resistance to tomato yellow leaf curl virus and *Ralstonia solanacearum*, respectively (Zamir et al., 1994; Thoquet et al., 1996), also map to this region. Only *Cf-2* and *Cf-5* have been cloned and encode receptors with N-terminal LRR regions and transmembrane domains, suggesting that R genes with distinct motifs are also clustered (Dixon et al., 1996, 1998).

Because members of distinct classes of R genes could be clustered in the same chromosomal region, identifying which type of R gene confers resistance to a specific pathogen requires extensive fine mapping, and, possibly, transforming more than one R gene type into susceptible genotypes to identify the gene in question. Recent development of virus-induced gene silencing (VIGS) technology allows assessment of the functional role of genes by targeting their transcripts for degradation (Lu et al., 2003; Burch-Smith et al., 2004). This technique also could be used to target members of a gene family by eliminating functional redundancy and correlating their roles to a specific function. Alternatively, this approach could be used to assess whether a novel function is conferred by a member or members of a known gene family. In this article, we describe the use of VIGS to assess whether the heat-stable root-knot nematode R gene *Mi-9* is a *Mi-1* homolog. We use the word homolog as an inclusive term to refer to orthologs or paralogs. First, we describe a molecular genetic analysis of the *Mi-9* region on the short arm of *S. arcanum* chromosome 6. We then identified *Mi-1* homologs in the *Mi-9* donor *S. arcanum* accession LA2157 that cosegregate with the heat-stable nematode resistance. Using VIGS targeted to silence *Mi-1* homologs in *S. arcanum* LA2157, we showed that *Mi-9* is likely a homolog of *Mi-1*.

RESULTS

Identifying Recombinants in the *Mi-9* Region

Earlier, *Mi-9* was mapped between markers CT119 and C8B, located on the telomeric distal end and

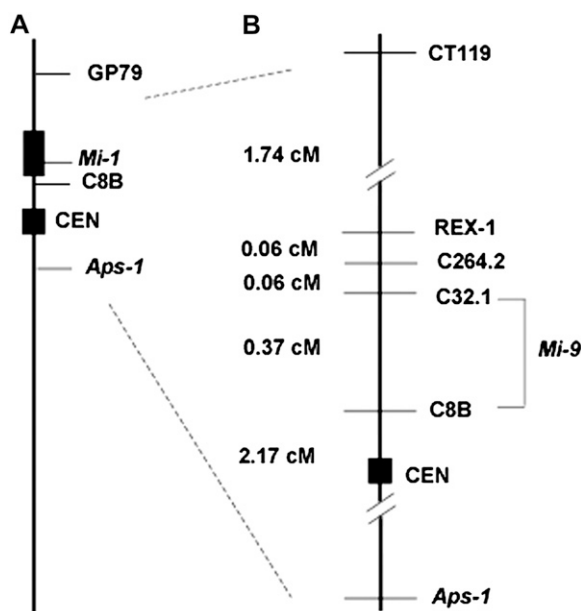


Figure 1. Genetic map of *Mi-1* and *Mi-9* on the short arm of tomato chromosome 6. A, *Mi-1* location and flanking markers. Thick bar represents the introgressed region from *S. peruvianum* in the tomato cv Motelle. B, *Mi-9* linkage map on the short arm of chromosome 6 generated by the mapping population *S. arcanum* accessions LA2157 × LA392. Numbers on the left of the vertical line indicate genetic distances (centimorgans).

centromeric proximal end of the short arm of chromosome 6, respectively (Fig. 1A). To further delimit the *Mi-9* location, we screened the F_2 population used previously and derived from a cross between the heat-stable root-knot nematode resistance *S. arcanum* accession LA2157 and the root-knot nematode susceptible accession LA392 (Ammiraju et al., 2003). A total of 589 F_2 progeny plants were scored for DNA markers CT119, Rex-1, C8B, and *Aps-1* (Supplemental Table S1). Segregation ratios for CT119, Rex-1, and *Aps-1* codominant markers were in agreement with the expected 1:2:1 ratios ($P = 0.40$ for CT119, $P = 0.85$ for Rex-1, and $P = 0.36$ for *Aps-1*).

Fifty-four recombinants were identified that had recombination between CT119 and *Aps-1* (Table I). All F_2 recombinants had a single recombination event. The largest group of recombinants, with 30 members, had a recombination event between *Aps-1* and C8B (F_2 classes 4–7; Table I). Within this group, the recombinant F_2 class 5 separated *Aps-1* and the heat-stable nematode resistance and localized *Mi-9* above *Aps-1*, confirming the earlier finding. This finding was further supported by F_3 segregation analysis of F_2 families in class 4 and class 5. Heat-stable nematode resistance in the F_3 populations from these families segregated in a 3 resistant:1 susceptible ratio as expected based on χ^2 statistics (Supplemental Table S2). Initially, while performing F_3 segregation marker analysis, we noticed unexpected segregation in F_3 plants that originated from a single F_2 fruit. We interpreted the surprising segregation results

as the ability of our *S. arcanum* population to both self fertilize and outcross. To make sure the F_3 seeds were from selfed F_2 plants, immature flowers on F_2 plants were bagged, and seeds from a single fruit were germinated and segregation of plants from the fruit was monitored.

Seventeen recombinants (F_2 classes 11–14; Table I) were identified between CT119 and Rex-1, and 16 of these recombinants (F_2 classes 11, 12, and 14) separated CT119 from *Mi-9* and localized *Mi-9* to the centromeric proximal end of the arm. Two additional RFLP markers, C264.1 and C32.1, located on the short arm of chromosome 6, were used to further map the recombinants (Table I; Kaloshian et al., 1998). One recombinant from F_2 class 10, E27, had recombination between Rex-1 and C264.1 (Table I), and F_3 progeny of this family segregated in a 3:1 ratio for heat-stable resistance (Supplemental Table S2), indicating that *Mi-9* is located below Rex-1 (e.g. E27-H3, Fig. 2; Supplemental Table S3). One recombinant (F_2 class 9; Table I) was also identified between markers C264.1 and C32.1, indicating that *Mi-9* is located below C264.1. Five recombinants were identified between C32.1 and C8B (F_2 class 8; Table I). The F_3 population from these F_2 families segregated in a 3 resistant:1 susceptible ratio for heat-stable resistance (Supplemental Table S2). Segregation analysis in four of these families (E42, R26, D52, and R35) indicated recombination between C8B and *Mi-9*, localizing *Mi-9* above C8B in agreement with our earlier finding (Supplemental Tables S2 and S3). The F_3 segregation of one of the F_2 families (A56) in this class (e.g. A56-E3; Fig. 2) did not separate *Mi-9* from C8B and localized *Mi-9* below C32.1, further delimiting the location of *Mi-9* on the centromeric proximal end of the short arm of chromosome 6. A genetic map of the *Mi-9* region was developed by combining the F_2 segregation data from this work and our previous results (Fig. 1, A and B).

Identification of R Gene Homologs on the Short Arm of Chromosome 6

Members of two distinct classes of R genes are localized to the short arm of chromosome 6 (Ho et al., 1992; Dickinson et al., 1993). These are the *Mi-1* gene with coiled coil-NBS-LRR protein motifs and *Cf-2* and *Cf-5* genes with transmembrane and LRR protein motifs (Dixon et al., 1996, 1998). We developed markers for *Cf-2* and *Mi-1* and assessed whether *Cf-2* or *Mi-1* homologs cosegregated with the heat-stable nematode resistance. The *Cf-2* primers amplified a fragment of 540 bp in both LA2157 and LA392 (Supplemental Table S1). Restriction with *TaqI* distinguished the two alleles by cleaving the amplified product from LA392 into two fragments of 380 bp and 160 bp, while the amplification product from LA2157 remained uncut (data not shown).

Mi-1 and six homologs are localized to the short arm of tomato chromosome 6 (Seah et al., 2004). To distinguish among *Mi-1* homologs, primers Mint-up and

Table 1. Segregation of *Mi-9* phenotype and linked markers in F_2 population of *S. arcanum* LA2157 \times LA392

Plants were genotyped using PCR and RFLP markers. Genotype designation: (1) homozygous resistant locus, (2) homozygous susceptible, (3) heterozygous, 1/3 resistant allele is dominant, and 2/3 susceptible allele is dominant. Plants were also evaluated for nematode resistance (R) or susceptibility (S) to root-knot nematodes strain VW4 at 32°C.

Plant	Attributes	No. of Plants	Phenotype	Markers							
				CT119	Cf-2	Rex-1	C264.1	C32.1	C8B	Aps-1	
LA2157	Parent	–	R	1	1	1	1/3	1	1/3	1	
LA392	Parent	–	S	2	2	2	2	2/3	2	2	
F_2 class 1	Parental type	124	R	1	1	1	nd ^a	nd	1/3	1	
F_2 class 2	Parental type	145	S	2	2	2	nd	nd	2	2	
F_2 class 3	Heterozygote	264	R	3	3	3	nd	nd	1/3	3	
F_2 class 4	Recombinant	6	R	3	3	3	1/3	2/3	3 ^b	1	
F_2 class 5	Recombinant	8	R	3	3	3	1/3	2/3	3 ^b	2	
F_2 class 6	Recombinant	5	S	2	2	2	2	2/3	2	3	
F_2 class 7	Recombinant	11	R	1	1	1	1/3	1/1	1 ^b	3	
F_2 class 8	Recombinant	5	R	3	3	3	1/3	2/3	1 ^b	1	
F_2 class 9	Recombinant	1	R	2	2	2	2	3 ^b	3 ^b	3	
F_2 class 10	Recombinant	1	R	1	1	1	3 ^b	3 ^b	3 ^b	3	
F_2 class 11	Recombinant	8	R	2	2	3	1/3	2/3	3 ^b	3	
F_2 class 12	Recombinant	2	S	3	3	2	2	2/3	2	2	
F_2 class 13	Recombinant	1 ^c	R	1	3	3	nd	nd	1/3	3	
F_2 class 14	Recombinant	6	R	2	3	3	nd	nd	1/3	3	

^and, Not determined.

^bAllele designation is based on F_3 progeny segregation.

^cPlant died before setting fruits.

Mint-do were designed that annealed to the intron 1 flanking regions (Fig. 3A). Using these primers in PCR with DNA from tomato containing *Mi-1*, we were able to amplify intron 1 from *Mi-1.1* and *Mi-1* (Supplemental Fig. S1). The size of the amplified fragments from *Mi-1.1* and *Mi-1* were 622 and 1,372 bp, respectively. We used intron 1 flanking primers in PCR with DNA from the source of *Mi-9*, LA2157, and four DNA fragments were amplified (Fig. 3B). We refer to these fragments as *RH1*, *RH2*, *RH3*, and *RH4* with sizes 1,372, 844, 786, and 756 bp, respectively. Using the intron 1 primers in PCR with DNA from LA392, the susceptible parent in our genetic cross, three distinct fragments, *SH1*, *SH2*, and *SH3*, with sizes 1,235, 713, and 556, respectively, were amplified (Fig. 3B).

To determine the number of *Mi-1* homologs in LA2157, DNA-blot analyses were performed using the NBS fragment from *Mi-1* as a probe. The DNA-blot analysis indicated the presence of about six to seven *Mi-1* homologs in LA2157 (Fig. 4).

Mapping *Cf-2* and *Mi-1* Homologs on Chromosome 6

We scored the entire F_2 population for *Cf-2* alleles and identified 10 recombinants between *Cf-2* and Rex-1 (F_2 classes 11 and 12; Table I) localizing *Cf-2* above Rex-1 to the telomeric distal end of the chromosome. In addition, seven recombinants were identified between *Cf-2* and CT119 (F_2 classes 13 and 14; Table I) localizing *Cf-2* below CT119. Because all members of the recombinant F_2 class 11 had heat-stable nematode resistant phenotype, this suggested that *Mi-9* is not likely to be a *Cf-2* homolog.

The segregation of *Mi-1* homologs was determined in over 289 F_2 plants that included all recombinant

plants. All tested nematode resistant F_2 plants with homozygous LA2157 markers located on the short arm of chromosome 6 displayed the four alleles from LA2157 (Supplemental Fig. S1). Moreover, all tested susceptible F_2 plants homozygous for LA392 markers in this region displayed the three alleles from LA392 (Supplemental Fig. S1), and all tested heterozygous F_2 plants displayed all seven members (data not shown). Taken together, these data suggest that the four *Mi-1* homologs from LA2157 and the three homologs from LA392 are localized to the short arm of chromosome 6. This was further confirmed using the recombinants.

The recombinants in F_2 classes 4, 5, 8, 11, and 14 displayed all seven *Mi-1* homologs (class 4 and 5, data not shown; e.g. E42 and A56 class 8, I47 class 11, 188 class 14; Fig. 3B). All recombinants in F_2 class 7 had LA2157 *Mi-1* alleles, while all recombinants in the F_2 class 6 had LA392 *Mi-1* alleles (data not shown). Crossover events among the *Mi-1* homologs were identified in members of the F_2 classes 8 to 10 and class 12. F_3 segregation of four of the F_2 class 8 families (E42-A4, R26-D6, D52-B5, and R35-B1; Supplemental Table S3; e.g. E42-A4, Figs. 2 and 3B) indicated that the recombination points are between C32.1 and C8B and that all seven *Mi-1* alleles are located above C8B (Fig. 2). Segregation of the F_3 population (e.g. A56-E3) of one member of this class, A56, not only supported this finding but also separated *Mi-1* homolog *RH4* from the three other homologs, *RH1*, *RH2*, and *RH3*, from LA2157 (Figs. 2 and 3B). The location of *Mi-1* homologs *RH4* above C32.1 was further confirmed by segregation of homologs in A42 and E27-H3 (Figs. 2 and 3B). *Mi-1* homolog profiles in M59 and U4 further localized *RH4* between *Cf-2* and Rex-1 (Figs. 2 and 3B).

The recombination mapping also uncovered the crossover points among *Mi-1* homologs from LA392. Segregation of *Mi-1* homolog *SH3* in E27, E27-H3, and A42-D2 indicates that *SH3* is located below C32.1 (Figs. 2 and 3B), while *Mi-1* homolog profiles from M59-F4 and 188-D2 indicated that *SH1* and *SH2* are located above *Cf-2* (Figs. 2 and 3B).

Sequence Relationships of *Mi-1* Homologs

To identify the relationship among the *Mi-1* homologs in LA2157 and LA392, the seven amplified intron fragments were sequenced (Supplemental Fig. S2). Fragments representing *Mi-1.1* and *Mi-1* intron 1 amplified from cv Motelle were also sequenced. Phylogenetic analysis grouped the intron sequences to three distinct clades (Fig. 5). Introns *RH1* and *SH1* grouped with intron 1 from *Mi-1*, while *RH4*, *SH2*, and *SH3* grouped with intron 1 from *Mi-1.1* (Fig. 5). A third clade was denoted by *RH2* and *RH3*, and both members had higher sequence identity to *Mi-1.1* than *Mi-1*. Sequence analysis indicated over 99% and 78% sequence identity between *Mi-1* intron 1 and *RH1* and *SH1*, respectively. Sequence identity between *Mi-1.1* and *Mi-1* intron 1 was only 32%. In contrast, intron 1 sequence identity between *Mi-1.1* and *RH4*, *SH2*, and *SH3* ranged between 63% and 77% (Fig. 5). The striking difference among all the intron 1 sequences is the presence of indels scattered along intron 1. One major deletion of about 740 bp differentiates between *Mi-1* and the members in clade 2 and clade 3 (Fig. 5; Supplemental Fig. S2).

VIGS in *S. arcanum* LA2157

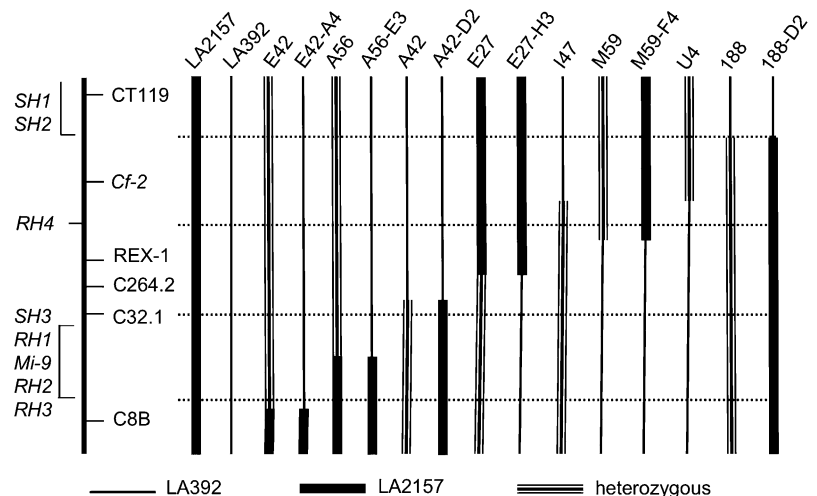
Mi-1 homologs cosegregated with the *Mi-9* heat-stable resistance, which suggested that *Mi-9* could be a homolog of *Mi-1*. To determine whether *Mi-9* is a homolog of *Mi-1*, we targeted transcripts of *Mi-1* homologs for degradation using tobacco (*Nicotiana tabacum*) rattle virus (TRV)-based VIGS. TRV is a bipartite virus

(TRV RNA1 [TRV1] and TRV RNA2 [TRV2]) and has been used effectively as a VIGS vector to silence genes in roots from Solanaceae (Ryu et al., 2004; Valentine et al., 2004). To examine whether TRV could be used efficiently to silence genes in *S. arcanum*, we infiltrated accession LA2157 with an *Agrobacterium* culture containing TRV1 and TRV2 carrying a fragment of tomato phytoene desaturase gene (TRV-*PDS*; Liu et al., 2002). Because temperature has an effect on the efficiency of VIGS in tomato (Ekengren et al., 2003), we tested TRV-VIGS at 19°C and 24°C. All LA2157 plants infiltrated with TRV-*PDS* and maintained at 19°C showed photo-bleaching symptoms (Supplemental Fig. S3A), while only 22% of the infiltrated plants maintained at 24°C showed the symptoms. Silencing within a plant was also more efficient when plants were maintained at 19°C compared to 24°C (Supplemental Fig. S3B).

Silencing of *Mi-1* Homologs in Accession LA2157 Using TRV-VIGS

To target *Mi-1* homologs in VIGS, a TRV-*Mi* clone was used (Li et al., 2006). Seedlings of LA2157 and tomato cv Motelle agroinfiltrated with empty vector TRV, TRV-*Mi* construct, or buffer controls were assayed for heat-stable root-knot nematode resistance at 32°C. Tomato cv Motelle was used as a positive control for *Mi-1*-mediated nematode resistance breakdown at high temperature. Eight weeks after nematode inoculation, egg masses developed on roots of tomato cv Motelle infiltrated with buffer, indicating success in breaking the *Mi-1*-mediated resistance (Fig. 6A). In addition, similar numbers of egg masses were developed on Motelle treated with buffer or agroinfiltrated with an empty TRV vector, indicating that *Agrobacterium* culture and/or TRV did not interfere with nematode infection. All LA2157 plants infiltrated either with buffer or TRV developed low numbers of egg masses, indicating that *Mi-9*-mediated heat-stable resistance is functional in these plants and that *Agrobacterium*

Figure 2. Genetic map of *Mi-9* and key *S. arcanum* recombinants. A map of the short arm of chromosome 6 is shown on the left. *Mi-1* homologs *RH1*, *RH2*, *RH3*, and *RH4* are from *S. arcanum* accession LA2157, while *SH1*, *SH2*, and *SH3* are from accession LA392. The region in *S. arcanum* from accession LA2157 is represented by vertical thick bar, from accession LA392 is represented by vertical thin bar, and heterozygous region is represented by vertical multiple line bar. In recombinants, junctions between regions are depicted as midway between flanking markers.



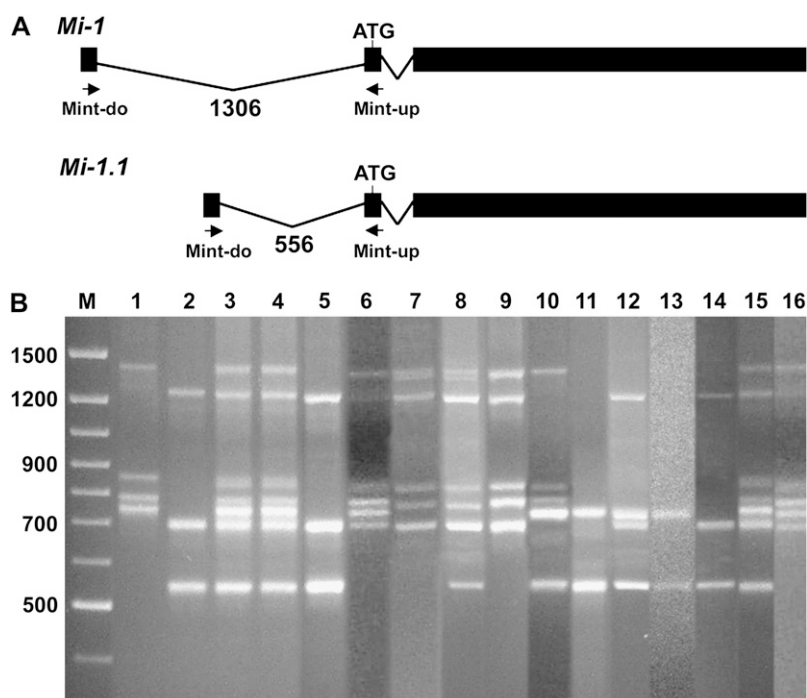


Figure 3. *Mi-1* and homologs in *Solanum* spp. A, Schematic diagram of *Mi-1* and *Mi-1.1* genes showing the relative positions of intron 1 flanking primers Mint-do and Mint-up (arrows). Thick horizontal lines represent transcripts and angled lines indicate introns. B, A composite image of *Mi-1* homologs amplified using PCR and intron 1 flanking primers and resolved on 2% agarose gels. DNA source in lanes 1 to 16 are from: LA2157, LA392, I47, E42, E42-A4, A56, A56-E3, A42, A42-D2, E27, E27-H3, M59, M59-F4, U4, 188, and 188-D2.

and/or TRV did not hinder *Mi-9*-mediated resistance. In contrast, a subset of LA2157 plants agroinfiltrated with the *Mi-1* VIGS construct developed large numbers of egg masses, indicating attenuation of *Mi-9*-mediated heat-stable resistance.

Root sections of LA2157 agroinfiltrated with the *Mi-1* VIGS construct and harboring egg masses were collected for RNA extraction and used in qualitative evaluation of the relative abundance of *Mi-1* transcripts. RNAs from five different roots were subjected to reverse transcription (RT)-PCR analysis using *Mi-1* primers (Li et al., 2006). All indicated reduction in *Mi-1* transcript levels compared to TRV only agroinfiltrated plants (Fig. 6B). Sequence information of RT-PCR product from uninfected LA2157 root RNAs indicated that six *Hmr1* (for homologs of Meloidogyne resistance gene *Mi-1*) transcripts were amplified with the *Mi-1* primers (Supplemental Fig. S4).

DISCUSSION

In this article, we report that the heat-stable root-knot nematode resistance gene *Mi-9* is a homolog of *Mi-1*. Our strategy was based on a combination of candidate gene approach and functional analysis without cloning. The short arm of tomato chromosome 6 is a rich source of disease R genes, and two distinct R gene groups have been cloned from this portion of the chromosome. These are *Cf-2* and *Cf-5* with LRR and transmembrane domains and *Mi-1* with NBS-LRR domains (Dixon et al., 1996, 1998; Kaloshian et al., 1998; Milligan et al., 1998). We considered the possi-

bility that either a homolog of *Cf* or *Mi-1* could confer the heat-stable nematode resistance. Fine mapping ruled out the possibility of a *Cf* homolog in this role. Because *Mi-1* homologs are clustered in two distinct groups, an easily distinguishable feature among *Mi-1* homologs was necessary to further map and identify the source of resistance. Only members of the cluster at the centromeric proximal end that included *Mi-1*, *Mi-1.1*, and *Mi-1.3* have been cloned and sequenced (Milligan et al., 1998). The feature that clearly distinguished between *Mi-1* and *Mi-1.1* was the size of the first intron. Furthermore, our work indicated that the size of intron 1 also allowed the distinction of several *Mi-1* homologs in *S. arcanum* accessions LA2157 and LA392. However, the PCR approach to amplify intron 1 did not detect all *Mi-1* homologs in either accession. DNA-blot analysis indicated the presence of five to seven *Mi-1* homologs in these accessions, and RT-PCR indicates six transcribed *Mi-1* homologs in LA2157 (Fig. 4; Supplemental Fig. S4). Nevertheless, the PCR approach allowed the distinction among seven *Mi-1* homologs and indicated that the intron 1 flanking sequences are conserved in four and three homologs from accessions LA2157 and LA392, respectively.

Our data indicated that three *Mi-1* homologs cosegregate with the heat-stable resistance in LA2157. However, it is not clear which one of the three members confers the heat-stable resistance and whether any of these members is a pseudogene. Although six distinct *Mi-1* homolog transcripts were identified in LA2157, a subset of these transcripts could be of pseudogene origin. Several *Mi-1* homologs are pseudogenes and are expressed in root-knot nematode susceptible and

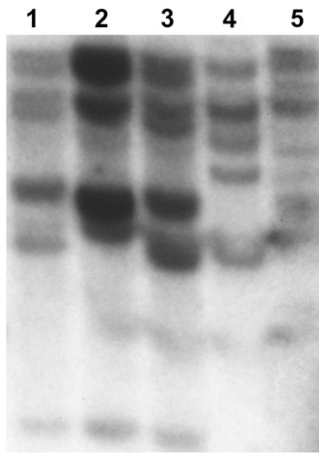


Figure 4. DNA-blot analysis of NBS fragment of *Mi-1*. Genomic DNA from tomato cv VFN (*Mi-1/Mi-1*; lane 1), cv UC82B (*mi/mi*; lane 2), cv Motelle (*Mi-1/Mi-1*; lane 3), *S. arcanum* accessions LA2157 (*Mi-9/Mi-9*; lane 4), and LA392 (*mi/mi*; lane 5) were digested with *EcoRV*, separated on 0.9% agarose gel, blotted onto nylon membrane, and hybridized with radiolabeled probe.

resistant tomato (S. Seah and V. M. Williamson, personal communication). In the *S. peruvianum* introgressed region, within the *Mi* locus at the centromeric proximal region, *Mi-1* and two homologs (*Mi-1.1* and *Mi-1.3*) are present. *Mi-1* and *Mi-1.1* have intron 1, but *Mi-1.3* does not have any detectable introns (Milligan et al., 1998). Although the primers used to amplify intron 1 will not identify members without introns, all three *Mi-1* homologs from LA2157 (*RH1*, *RH2*, and *RH3*) located in the centromeric proximal cluster have intron 1. However, phylogenetic analysis of the intron 1 sequences of *Mi-1.1*, *Mi-1*, and homologs from LA2157 and LA392 did not distinguish between members of the two clusters, indicating that extensive sequence exchange among homologs in these clusters has occurred.

S. peruvianum sensu lato is a heterogeneous species complex, and the northern races of this species were considered the ancestral progenitor of the *Solanum* complex (Rick, 1986; Spooner et al., 2005). Both parental accessions LA2157 and LA392 are from the northern races of *S. peruvianum* recently renamed as *S. arcanum* (Peralta et al., 2005). As demonstrated in this work, considerable polymorphism exists between these two accessions. However, our recombination analysis indicates that the marker order is consistent among these two *S. arcanum* accessions and the introgressed region in tomato from *S. peruvianum* (Kaloshian et al., 1998). *S. peruvianum s. str.* PI128657 is the accession that *Mi-1* was introduced from and was collected from the southern region of Peru (Veremis and Roberts, 2000). Comparing markers in the *Mi* region between *S. lycopersicum* and the *S. peruvianum* introgressed region, an inversion encompassing *Rex-1* and *C264.2* has been demonstrated (Seah et al., 2004). The presence of this inversion partly explains the lack of recombination in this region in crosses between root-knot nem-

atode susceptible tomato and resistant tomato that contains *S. peruvianum*-introgressed region (Kaloshian et al., 1998; Seah et al., 2004). Although the suppression of recombination is partly attributed to the presence of the *S. peruvianum*-introgressed genome, the suppression is more pronounced in the region spanning the inversion (Liharska et al., 1996; Kaloshian et al., 1998; Seah et al., 2004). While several recombination events were identified in close proximity to the *Mi* locus, no recombination between *C264.2* and *Rex-1* was previously reported (Kaloshian et al., 1998). Earlier, the order of these two markers was determined by a physical map using yeast artificial chromosomes and cosmid subclones (Kaloshian et al., 1998).

In this work, we identified a recombination event between these two markers that localized *Rex-1* above *C264.2* on the telomeric end of the short arm of chromosome 6, in agreement with the physical map of the *Mi-1* introgressed region. Because the *Rex-1* and *C264.2* positions are the same in *S. peruvianum* accession PI128657 and in *S. arcanum* accessions LA2157 and LA392, it is therefore likely that the inversion happened in *S. lycopersicum* after divergence from *S. peruvianum sensu lato*. Because the previous mapping information was from only one representative of each *S. lycopersicum* and *S. peruvianum* genomes, it was difficult to determine in which species the inversion happened (Seah et al., 2004).

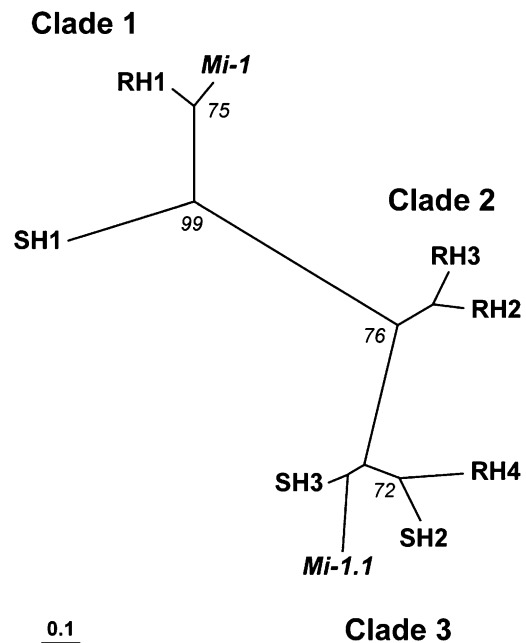


Figure 5. An unrooted parsimony tree showing the differentiation of the three groups of *Mi-1* intron 1 homologs. The phylogenetic analysis includes *Mi-1.1*, *Mi-1*, and homologs from *S. arcanum* accessions LA2157 (resistance parent homologs, *RH*) and LA392 (susceptible parent homologs, *SH*), namely *RH1* (EF028059), *RH2* (EF028056), *RH3* (EF028057), *RH4* (EF028058), *SH1* (EF028060), *SH2* (EF028061), and *SH3* (EF028062). Numbers at nodes represent bootstrap values. Scale bar indicates number of substitution per site.

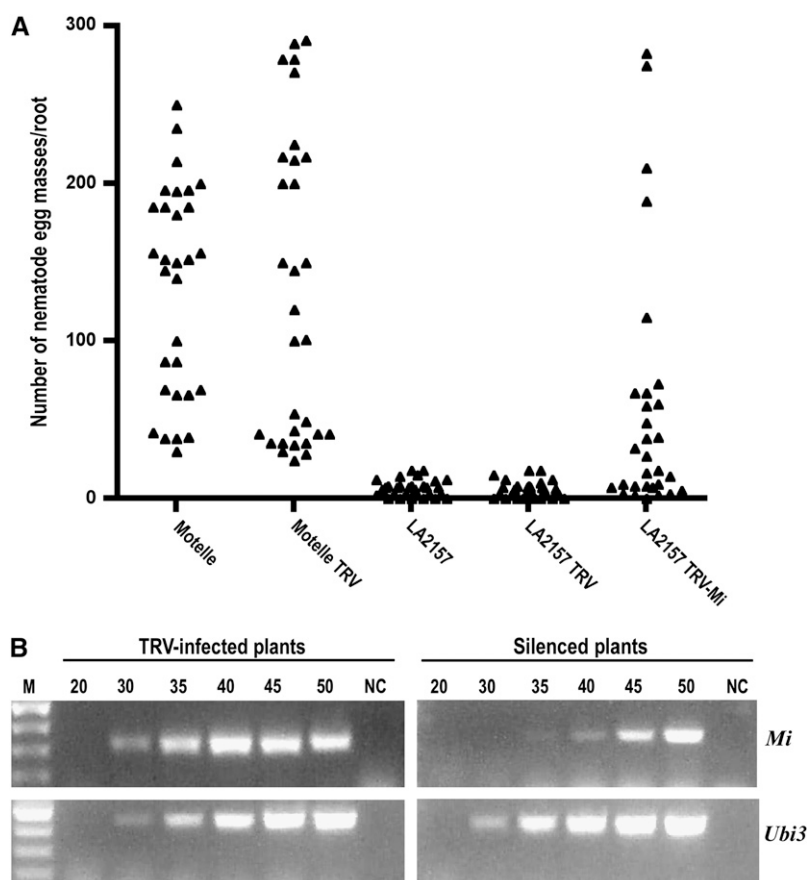


Figure 6. TRV-*Mi* VIGS attenuated *Mi-9*-mediated heat-stable root-knot nematode resistance in *S. arcanum* accession LA2157. **A**, Root-knot nematode infection on roots of buffer-infiltrated controls or agroinfiltrated with pTRV1 plus pTRV2 empty vector (TRV) or with pTRV1 plus pTRV2-*Mi* (TRV-*Mi*). Triangles represent number of egg masses per root system. Two independent experiments were performed. In each experiment, 15 plants per treatment were used. Data from both experiments are presented. **B**, Effect of TRV-*Mi* VIGS on *Mi-1* transcript levels in silenced and control roots. Ethidium bromide stained 1.5% agarose gels with RT-PCR products. cDNA was synthesized from total RNA isolated from roots of plants agroinfiltrated with TRV or TRV-*Mi*. Samples from TRV-*Mi* infiltrated plants were from roots portions supporting nematode reproduction. Amplification of the tomato ubiquitin *Ubi3* gene was used as an internal control for equal cDNA use from control and silenced plants. PCR cycles are as indicated on the top of the sections. Lane M indicates DNA marker, and NC indicates negative control where RNA was used as template in the absence of reverse transcriptase.

Our recombination data mapped CT119 above *Cf-2* in *S. arcanum*. In *Solanum pimpinellifolium*, the source of *Cf-2*, CT119 is localized below *Cf-2* (Dixon et al., 1995). *Cf-2* is a member of a gene family, and different numbers of homologs are reported from *S. lycopersicum*, which lacks *Cf-2*, compared to *S. pimpinellifolium*. In addition, the region spanning CT119 and *Cf-2* is about 30 kb in *S. lycopersicum* (Dixon et al., 1995, 1996). In our population, we identified seven recombinants between CT119 and *Cf-2*, suggesting that the member amplified in the *S. arcanum* in our experiments is different than the members in *S. pimpinellifolium*, and/or this region in *S. arcanum* encompasses a recombination hot spot.

We also demonstrated in this work that TRV can be used as a functional tool for VIGS in *S. arcanum*. TRV-VIGS is highly efficient in *S. arcanum* LA2157 where 100% of the plants infiltrated with TRV-*PDS* showed photo-bleaching symptoms. Along with *S. arcanum*, we also tested the efficiency of TRV-VIGS using TRV-*PDS* in *S. peruvianum* and *S. pimpinellifolium* and found high efficiency of silencing in both species (K. Bhattarai and I. Kaloshian, unpublished data). Although TRV-VIGS is highly efficient in LA2157, silencing is not uniform within a plant and within a single leaflet, as visualized by *PDS* silencing (Supplemental Fig. S3A). The patchy pattern of silencing of TRV-VIGS has also

been observed in above-ground parts of tomato (Liu et al., 2002; Ekengren et al., 2003). In TRV-*Mi* infiltrated roots, root-knot nematode egg masses were clustered in a limited number of patches on the root system, suggesting that the patchy nature of TRV-VIGS in below-ground parts (roots) mirrors the above-ground parts (shoots).

The observed variation in number of egg masses on roots of LA2157 is partly due to the variable efficiency of TRV-*Mi* silencing and efficiency of TRV-VIGS in roots (Valentine et al., 2004). Comparing TRV-*Mi* silencing in tomato leaves and roots using aphid and nematode assays, respectively, suggests that silencing in roots is less efficient than in leaves (I. Kaloshian, unpublished data). The ability of nematodes to infect and develop is based on interaction of the nematode with a few distinct root cells where feeding is initiated. If *Mi-9* is silenced in these cells, then the nematode is able to initiate successful parasitism and complete its life cycle. However, the absence of *Mi-9* silencing in even a few cells at the site of nematode feeding will inhibit parasitism. Variation in numbers of egg masses also could be due to high temperature breaking the *Mi-1*-mediated resistance. Variable numbers of egg masses were also observed in the Motelle infiltrated with buffer treatment, indicating that temperature may have played a role in nematode infectivity.

Combining a fine-mapping strategy, candidate gene approach with VIGS allowed us to determine the likely nature of *Mi-9* without cloning. The development of wide host range virus vectors such as TRV will facilitate the adoption of this approach to a wide variety of plant species and accelerate the identification of the nature of the R genes prior to cloning. This approach will be especially valuable in regions where R genes have been mapped and where clusters of R genes with distinct motifs reside. Because only 23 nucleotides identity is needed between the insert sequence in the VIGS vector and the targeted gene, VIGS will assist in quickly identifying the sequence motif of the R gene in question and result in targeting a limited number of candidate genes for stable transformation (Thomas et al., 2001). As plant genomes and EST databases are completed, TRV-VIGS could be used to target a specific member of a gene family by designing gene-specific VIGS constructs.

Heat instability of R genes is a feature of a number of root-knot nematode R genes from distinct plant families (Griffin, 1969; Jatala and Russell, 1972; Carter, 1982). Because *Mi-9* is a homolog of *Mi-1*, cloning *Mi-9* will assist in determining the nature of heat stability.

MATERIALS AND METHODS

Plants Material and Growth Conditions

Two accessions of *Solanum arcanum* (formerly *Lycopersicon peruvianum*), LA2157 and LA392, and three tomato (*Solanum lycopersicum*; formerly *Lycopersicon esculentum*) cultivars Motelle (*Mi-1/Mi-1*), VFN (*Mi-1/Mi-1*), and UC82B (*mi/mi*), were used in this study. Seeds were sown in seedling trays filled with organic planting mix (Sun Gro Horticulture). Two to 4 weeks after germination, seedlings were either used directly or transplanted into larger containers. To assist in uniform germination, seedling trays were maintained in a greenhouse in an enclosed structure with misters. Plants were maintained in a greenhouse at 22°C to 26°C unless otherwise stated. After germination, seedlings were supplemented with Osmocote (17-6-10; Sierra Chemical) and fertilized biweekly with tomato MiracleGro (18-18-21; Stern's MiracleGro Products).

Nematode Cultures

Cultures of *Mi-1*-avirulent *Meloidogyne incognita* isolate VW4 and Project 77 were maintained on tomato cv UC82B in a greenhouse. Eggs were extracted from infected roots by processing in 0.52% (v/v) NaOCl in a Waring blender for 2 min at high speed (Hussey and Barker, 1973). Eggs and root debris were collected on a 43- μ m pore diameter sieve. Infective stage juveniles (J2) were obtained by hatching the eggs, as described in Martinez de Ilarduya et al. (2001). J2 were collected every 48 h and used immediately or stored at room temperature for an additional 48 h with aeration.

Nematode Screens

Heat-stable resistance screens were carried out in growth chambers with 16-h-light and 8-h-dark photoperiod and 700 μ mol m⁻² s⁻¹ light intensity. Five to 6-week-old plants in 10-cm pots filled with steam-sterilized loamy sand were used in these assays. Plants were moved to the growth chamber set at 25°C. The temperature in the chamber was raised gradually over a 2-d period to 32°C. Plants were maintained at 32°C for 2 to 3 d before inoculation. Plants were inoculated with 3,000 J2 and maintained at 32°C for 4 weeks. Plants were then moved to a greenhouse and maintained at 22°C to 26°C for three additional weeks. For F₃ screens, 12 to 22 F₃ individuals were used per F₂ family.

Eight weeks after inoculation, nematode reproduction was evaluated by staining roots in 0.001% (w/v) erioglaucine (Sigma-Aldrich). Plants were classified as resistant if the individual root system had less than 20 egg masses, or susceptible if the individual root system had 25 or more egg masses. Susceptible tomato cultivar UC82B was included as control for nematode infectivity, and *Mi-1*-containing cultivars VFN or Motelle were included as controls for breakdown of *Mi-1*-mediated resistance.

DNA Isolation and DNA-Blot Analysis

For PCR analyses, DNA was isolated from leaflets using Wizard Genomic DNA purification kit (Promega) according to manufacturer's recommendation or as described in Ammiraju et al. (2003). For DNA-blot analysis, DNA was isolated, restricted with *EcoRV* restriction enzyme, and DNA blots prepared according to Kaloshian et al. (1998). A 300-bp subclone of *Mi-1* containing the NBS region (clone 3-3) was used as probe. The random-primed ³²P-labeled probe was prepared from insert amplified from plasmid DNA using PCR. Hybridization was carried out overnight in 50% (v/v) formamide at 42°C, and final washes were done in 0.5× SSC, 0.1% (w/v) SDS at 48°C.

PCR-Based Markers

Aps-1, *Rex-1*, *CT119*, and *C8B* PCR-based markers and conditions used for these markers were described previously (Dixon et al., 1995; Kaloshian et al., 1998; Ammiraju et al., 2003).

Primers were developed to amplify *Cf-2.1* (Supplemental Table S1). To distinguish among *Mi-1* homologs, we made use of a unique feature that distinguishes between the functional *Mi-1* gene and its homolog *Mi-1.1*. Both *Mi-1* and *Mi-1.1* have two introns. While the size of intron 2 is similar in both genes, the size of intron 1 is variable, 556 bp in *Mi-1.1* and 1,306 bp in *Mi-1* (Milligan et al., 1998). The sequences flanking intron 1 in both *Mi-1.1* and *Mi-1* are identical. To amplify intron 1, primers were designed that annealed to the intron-flanking regions. The primers are Mint-do, 5'-TTCTCTAGCTAAACTT-CAGCC-3' and Mint-up, 5'-TTTTTCGTTTTCCATGATTCTAC-3'. Mint-do primer annealed to nucleotides 1,280 to 1,300 of *Mi-1* (GenBank accession no. U65668) and 1,045 to 1,065 of *Mi-1.1* (GenBank accession no. U65667), and Mint-up primer annealed to nucleotides 2,629 to 2,651 of *Mi-1* and 1,644 to 1,666 of *Mi-1.1*. PCR conditions were as described for *Rex-1*, except 3 mM MgCl₂ was used. Products were resolved on 1.5% to 2% (w/v) agarose gels.

Sequence Analysis

Nucleotide alignments were performed using ClustalX (Thompson et al., 1997) and edited manually using GENEDOC (<http://www.psc.edu/biomed/genedoc>). For intron 1 data, intron/exon boundaries were determined based on *Mi-1* cDNA sequence information, and intron sequences were used to generate phylogenetic trees using parsimony and maximum likelihood methods in PAUP 4.0 (Sinauer Associates). The HKY + G likelihood model for the intron 1 data matrix was chosen using Winmodeltest (Posada and Crandall, 1998). The parsimony tree was obtained by using a heuristic search implemented in PAUP. Bootstrap value for each node was calculated from 3,000 replicates. Maximum likelihood analysis was similarly conducted with heuristic search using the model defined for the data matrix.

RNA Isolation and RT-PCR

Total RNA was extracted using Trizol (Invitrogen) according to manufacturer's recommendation. Five micrograms of total RNA was treated with 1 unit RNase-free DNase I (Promega), and cDNAs were synthesized as described in Li et al. (2006). In PCR, *Mi-1* transcripts were amplified using primers VIGS-F, 5'-CTGCGTCTACTGACTCTTCC-3' and C2S4, 5'-CTAAG-AGGAATCTCATCACAGG-3', and tomato ubiquitin *Ubi3* gene transcripts were amplified as an internal control for equal cDNA use from control and silenced plants, as described in Li et al. (2006). To confirm lack of genomic DNA contamination, 200 ng of DNase-treated RNAs were also used as template. High fidelity Platinum Taq DNA polymerase (Invitrogen) was used. The amplified products were analyzed on 1.5% (w/v) agarose gels stained with ethidium bromide, gel purified, and ligated into a TOPO TA cloning vector (Invitrogen). Two independent RT-PCR reactions were performed and cloned. At least 15 recombinant plasmids were sequenced from each cloning.

Virus Constructs Used in VIGS

The TRV vector used in these experiments was previously described (Liu et al., 2002). The TRV-*PDS* construct was a gift from Dr. Dinesh-Kumar (Yale University). The TRV-*Mi* construct was engineered by cloning a 300-bp *Mi-1* cDNA fragment spanning the carboxy terminal end of the *Mi-1* gene and amplified using primers C1/2Do and C2S4 into pTRV2, as described in Li et al. (2006). The resulting plasmid was transformed into *Agrobacterium tumefaciens* strain GV3101.

Agrobacterium-Mediated Virus Infection

One-milliliter cultures of *A. tumefaciens* strain GV3101 containing each of the constructs derived from pTRV2, empty vector control, and pTRV1 were grown overnight in Luria-Bertani medium containing 50 $\mu\text{g mL}^{-1}$ kanamycin and 12.5 $\mu\text{g mL}^{-1}$ rifampicin at 28°C. Each overnight culture was used to inoculate 50-mL cultures of Luria-Bertani medium containing the same antibiotics, 10 mM MES, and 20 μM acetosyringone. The cultures were grown overnight at 28°C. *Agrobacterium* cultures were pelleted, resuspended in infiltration buffer (10 mM MgCl_2 , 10 mM MES, and 200 μM acetosyringone), and adjusted to an OD_{600} value of 0.8. Bacteria were incubated at room temperature for 3 h before use. An equal volume of pTRV1 *Agrobacterium* culture was mixed with pTRV2-*PDS* or pTRV2-*Mi* cultures before infiltration.

The abaxial side of leaflets of 4-week-old seedlings was infiltrated with *A. tumefaciens* cells (agroinfiltration) using a 3-mL needleless syringe. Seedlings were maintained at either 19°C or 24°C in growth chambers. Ten days after infiltration, seedlings used in nematode resistance assays were transplanted into plastic cups (10 cm diameter, 17 cm deep) filled with sand. Plants were maintained at 19°C for 10 additional days before nematode inoculation.

Sequence data from this article can be found in the GenBank/EMBL data libraries under accession numbers EF028056 to EF028062.

Supplemental Data

The following materials are available in the online version of this article.

Supplemental Figure S1. Distinct *Mi-1* homologs cosegregate with resistant and susceptible phenotypes in F_2 population of *S. arcanum* accessions LA2157 \times LA392.

Supplemental Figure S2. Alignment of *Mi* intron 1 amplified using Mint-up and Mint-do primers from *S. arcanum* accessions LA2157 and LA392.

Supplemental Figure S3. TRV-mediated silencing in *S. arcanum* accession LA2157.

Supplemental Figure S4. Alignment of *Hmr1* (for homologs of *Meloidogyne* resistance gene *Mi-1*) sequences.

Supplemental Table S1. Genetic analysis of F_3 progeny.

Supplemental Table S2. Characteristics of PCR markers and respective primers.

Supplemental Table S3. Segregation of *Mi-9* phenotype, *Mi-1* homologs, and linked markers in parents and key recombinants.

ACKNOWLEDGMENTS

We thank Drs. Paul Deley and Cheryl Hayashi for help with phylogenetic analysis, Scott Edwards for help with figures, and Qi Li, Daniela Noyes, Amal Khoury, Debrina Johnson, and Yaya Mansour for technical assistance. We are also grateful to Dr. Valerie M. Williamson, University of California, Davis, for sharing unpublished data.

Received September 7, 2006; accepted December 8, 2006; published December 15, 2006.

LITERATURE CITED

Ammati M, Thomason IJ, McKinney HE (1986) Retention of resistance to *Meloidogyne incognita* in *Lycopersicon* genotypes at high soil temperature. *J Nematol* 18: 491–495

Ammati M, Thomason IJ, Roberts PA (1985) Screening *Lycopersicon* spp. for new genes imparting resistance to root-knot nematodes (*Meloidogyne* spp.). *Plant Dis* 69: 112–115

Ammiraju JS, Veremis JC, Huang X, Roberts PA, Kaloshian I (2003) The heat-stable root-knot nematode resistance gene *Mi-9* from *Lycopersicon peruvianum* is localized on the short arm of chromosome 6. *Theor Appl Genet* 106: 478–484

Atherton JG, Rudich J (1986) *The Tomato Crop. A Scientific Basis for Improvement*. Chapman and Hall, New York

Bai YL, van der Hulst R, Bonnema G, Marcel BC, Meijer-Dekens F, Niks RE, Lindhout P (2005) Tomato defense to *Oidium neolycoopersici*: dominant *Ol* genes confer isolate-dependent resistance via a different mechanism than recessive *ol-2*. *Mol Plant Microbe Interact* 18: 354–362

Bendahmane A, Kanyuka K, Baulcombe DC (1999) The *Rx* gene from potato controls separate virus resistance and cell death responses. *Plant Cell* 11: 781–792

Burch-Smith TM, Anderson JC, Martin GB, Dinesh-Kumar SP (2004) Applications and advantages of virus-induced gene silencing for gene function studies in plants. *Plant J* 39: 734–746

Cap GB, Roberts PA, Thomason IJ (1993) Inheritance of heat-stable resistance to *Meloidogyne incognita* in *L. peruvianum* and its relationship to the *Mi* gene. *Theor Appl Genet* 85: 777–783

Carter WW (1982) Influence of soil temperature on *Meloidogyne incognita* on resistant and susceptible cotton. *J Nematol* 14: 343–346

Dickinson MJ, Jones DA, Jones JDG (1993) Close linkage between the *Cf-2/Cf-5* and *Mi* resistance loci in tomato. *Mol Plant Microbe Interact* 6: 341–347

Dixon MS, Hatzixanthos K, Jones DA, Harrison K, Jones JDG (1998) The tomato *Cf-5* disease resistance gene and six homologs show pronounced allelic variation in leucine-rich repeat copy number. *Plant Cell* 105: 1915–1925

Dixon MS, Jones DA, Hatzixanthos K, Ganai MW, Tanksley SD, Jones JDG (1995) High-resolution mapping of the physical location of the tomato *Cf-2* gene. *Mol Plant Microbe Interact* 8: 200–206

Dixon MS, Jones DA, Keddie JS, Thomas CM, Harrison K, Jones JDG (1996) The tomato *Cf-2* disease resistance locus comprises two functional genes encoding leucine-rich repeat proteins. *Cell* 84: 451–459

Dropkin VH (1969a) Cellular responses of plants to nematode infections. *Annu Rev Phytopathol* 7: 101–122

Dropkin VH (1969b) The necrotic reaction of tomatoes and other hosts resistant to *Meloidogyne*: reversal by temperature. *Phytopathology* 59: 1632–1637

Ekengren SK, Liu Y, Schiff M, Dinesh-Kumar SP, Martin GB (2003) Two MAPK cascades, *NPR1*, and *TGA* transcription factors play a role in *Pto*-mediated disease resistance in tomato. *Plant J* 36: 905–917

Griffin GD (1969) Effects of temperature on *Meloidogyne hapla* in alfalfa. *Phytopathology* 59: 599–609

Ho J-Y, Weide R, Ma HM, Wordragen ME, Lambert KN, Koornneef M, Zabel P, Williamson VM (1992) The root-knot nematode resistance gene (*Mi*) in tomato: construction of a molecular linkage map and identification of dominant cDNA markers in resistant genotypes. *Plant J* 2: 971–982

Holtzmann OV (1965) Effects of soil temperature on resistance of tomato to root-knot nematode (*Meloidogyne incognita*). *Phytopathology* 55: 990–992

Hussey R, Barker KR (1973) A comparison of methods of collecting inocula of *Meloidogyne* species including a new technique. *Plant Dis Rep* 57: 1025–1028

Jatala P, Russell CC (1972) Nature of sweet potato resistance to *Meloidogyne incognita* and the effects of temperature on parasitism. *J Nematol* 4: 1–7

Johnson AW (1998) Vegetable crops. In G Pederson, G Windham, K Barker, eds, *Plant-Nematode Interactions*. Agronomy Society of America, Madison, WI, pp 595–635

Kaloshian I, Yaghoobi J, Liharska T, Hontelez J, Hanson D, Hogan P, Jesse T, Wijbrandi J, Simons G, Vos P, et al (1998) Genetic and physical localization of the root-knot nematode resistance locus *Mi* in tomato. *Mol Gen Genet* 257: 376–385

Kesseli RV, Paran I, Michelmore RW (1994) Analysis of a detailed genetic linkage map of *Lactuca sativa* (lettuce) constructed from RFLP and RAPD markers. *Genetics* 136: 1435–1446

Li Q, Xie Q-G, Smith-Becker J, Navarre D, Kaloshian I (2006) *Mi-1*-mediated aphid resistance involves salicylic acid and mitogen-activated protein kinase signaling pathways. *Mol Plant Microbe Interact* 19: 655–664

- Liharska TB, Koornneef M, van Wordragen M, van Kammen A, Zabel P** (1996) Tomato chromosome 6: effect of alien chromosomal segments on recombinant frequencies. *Genome* **39**: 485–491
- Liu Y, Schiff M, Dinesh-Kumar SP** (2002) Virus-induced gene silencing in tomato. *Plant J* **31**: 777–786
- Lu R, Martin-Hernandez AM, Peart JR, Malcuit I, Baulcombe DC** (2003) Virus-induced gene silencing in plants. *Methods* **30**: 296–303
- Martinez de Ilarduya O, Moore AE, Kaloshian I** (2001) The tomato *Rme1* locus is required for *Mi-1*-mediated resistance to root-knot nematodes and the potato aphid. *Plant J* **27**: 417–425
- Meyers BC, Chin DB, Shen KA, Sivaramkrishnan S, Lavelle DO, Zhang Z, Michelmore RW** (1998) The major resistance gene cluster in lettuce is highly duplicated and spans several megabases. *Plant Cell* **10**: 1817–1832
- Michelmore RW, Meyers BC** (1998) Clusters of resistance genes in plants evolve by divergent selection and birth-and-death process. *Genome Res* **8**: 1113–1130
- Milligan SB, Bodeau J, Yaghoobi J, Kaloshian I, Zabel P, Williamson VM** (1998) The root-knot nematode resistance gene *Mi* from tomato is a member of leucine zipper, nucleotide binding, leucine-rich repeat family of plant genes. *Plant Cell* **10**: 1307–1319
- Noel L, Moores TL, van Der Biezen EA, Parniske M, Daniels MJ, Parker JE, Jones JD** (1999) Pronounced intraspecific haplotype divergence at the *RPP5* complex disease resistance locus of Arabidopsis. *Plant Cell* **11**: 2099–2112
- Noling JW** (2000) Effects of continuous culture of resistant tomato cultivars on *Meloidogyne incognita* soil population density and pathogenicity. *J Nematol* **32**: 452
- Nombela G, Williamson VM, Muñiz M** (2003) The root-knot nematode resistance gene *Mi-1.2* of tomato is responsible for resistance against the whitefly *Bemisia tabaci*. *Mol Plant Microbe Interact* **16**: 645–649
- Parrella G, Moretti A, Gognalons P, Lesage ML, Marchoux G, Gebre-Selassie K, Caranta C** (2004) The *Am* gene controlling resistance to Alfalfa mosaic virus in tomato is located in the cluster of dominant resistance genes on chromosome 6. *Phytopathology* **94**: 345–350
- Peralta IE, Knapp SK, Spooner DM** (2005) New species of wild tomatoes (*Solanum* section *Lycopersicon*: Solanaceae) from Northern Peru. *Syst Bot* **30**: 424–434
- Peralta IE, Spooner DM** (2005) Morphological characterization and relationships of wild tomatoes (*Solanum* L. section *Lycopersicon*). *Monogr Syst Bot Missouri Bot Gard* **104**: 227–257
- Philis J, Vakis N** (1977) Resistance of tomato varieties to the root-knot nematodes *Meloidogyne javanica* in Cyprus. *Nematol Mediterr* **5**: 39–44
- Posada D, Crandall KA** (1998) MODELTEST: testing the model of DNA substitution. *Bioinformatics* **14**: 817–818
- Rick CM** (1979) Biosystematic studies in *Lycopersicon* and closely related species of *Solanum*. In JG Hawkes, RN Lester, AD Skelding, eds, *The Biology and Taxonomy of the Solanaceae*. Academic Press, London, pp 667–677
- Rick CM** (1986) Reproductive isolation in the *Lycopersicon peruvianum* complex. In WG D'Arcy, ed, *Solanaceae: Biology and Systematics*. Colombia University Press, New York, pp 477–495
- Roberts PA, May DM** (1986) *Meloidogyne incognita* resistance characteristics in tomato genotypes developed for processing. *J Nematol* **18**: 353–359
- Rossi M, Goggin FL, Milligan SB, Kaloshian I, Ullman DE, Williamson VM** (1998) The nematode resistance gene *Mi* of tomato confers resistance against the potato aphid. *Proc Natl Acad Sci USA* **95**: 9750–9754
- Ryu CM, Anand A, Kang L, Mysore KS** (2004) Agrodrench: a novel and effective agroinoculation method for virus-induced gene silencing in roots and diverse Solanaceous species. *Plant J* **40**: 322–331
- Sasser JN** (1980) Root-knot nematodes: a global menace to crop production. *Plant Dis* **64**: 36–41
- Seah S, Yaghoobi J, Rossi M, Gleason CA, Williamson VM** (2004) The nematode-resistance gene, *Mi-1*, is associated with an inverted chromosomal segment in susceptible compared to resistant tomato. *Theor Appl Genet* **108**: 1635–1642
- Spooner DM, Peralta IE, Knapp S** (2005) Comparison of AFLPs with other markers for phylogenetic inference in wild tomatoes (*Solanum* L. section *Lycopersicon* (Mill.) Wettst.). *Taxon* **54**: 43–61
- Thomas CL, Jones L, Baulcombe DC, Maule AJ** (2001) Size constraints for targeting post-transcriptional gene silencing and for RNA-directed methylation in *Nicotiana benthamiana* using a potato virus X vector. *Plant J* **25**: 417–425
- Thompson JD, Gibson TJ, Plewniak F, Jeanmougin F, Higgins DG** (1997) The CLUSTAL_X windows interface: flexible strategies for multiple sequence alignment aided by quality analysis tools. *Nucleic Acids Res* **25**: 4876–4882
- Thoquet P, Olivier J, Sperisen C, Rogowsky P, Prior P, Anais G, Mangin B, Bazin B, Nazer R, Grimsley N** (1996) Polygenic resistance of tomato plants to bacterial wilt in the French West Indies. *Mol Plant Microbe Interact* **9**: 837–842
- Tzortzakakis EG, Gowen SR** (1996) Occurrence of resistance breaking pathotypes of *Meloidogyne javanica* on tomatoes in Crete, Greece. *Fundam Appl Nematol* **19**: 283–288
- Valentine T, Shaw J, Blok VC, Phillips MS, Oparka KJ, Lacomme C** (2004) Efficient virus-induced gene silencing in roots using a modified tobacco rattle virus vector. *Plant Physiol* **136**: 3999–4009
- van der Vossen EA, van der Voort JN, Kanyuka K, Bendahmane A, Sandbrink H, Baulcombe DC, Bakker J, Stiekema WJ, Klein-Lankhorst RM** (2000) Homologues of a single resistance-gene cluster in potato confer resistance to distinct pathogens: a virus and a nematode. *Plant J* **23**: 567–576
- Veremis JC, Roberts PA** (1996a) Identification of resistance to *Meloidogyne javanica* in the *Lycopersicon peruvianum* complex. *Theor Appl Genet* **93**: 894–901
- Veremis JC, Roberts PA** (1996b) Relationships between *Meloidogyne incognita* resistance genes in *Lycopersicon peruvianum* differentiated by heat sensitivity and nematode virulence. *Theor Appl Genet* **93**: 950–959
- Veremis JC, Roberts PA** (2000) Diversity of heat-stable genotype specific resistance of *Meloidogyne* in Maranon races of *Lycopersicon peruvianum* complex. *Euphytica* **111**: 9–16
- Veremis JC, van Heusden AW, Roberts PA** (1999) Mapping a novel heat-stable resistance to *Meloidogyne* in *Lycopersicon peruvianum*. *Theor Appl Genet* **98**: 274–280
- Vos P, Simons G, Jesse T, Wijbrandi J, Heinen L, Hogers R, Frijters A, Groenendijk J, Diergaarde P, Reijans M, et al** (1998) The tomato *Mi-1* gene confers resistance to both root-knot nematodes and potato aphids. *Nat Biotechnol* **16**: 1365–1369
- Yaghoobi J, Kaloshian I, Wen Y, Williamson VM** (1995) Mapping a new nematode resistance locus in *Lycopersicon peruvianum*. *Theor Appl Genet* **91**: 457–464
- Zamir D, Eksteinmichelson I, Zakay Y, Navot N, Zeidan M, Sarfatti M, Eshed Y, Harel E, Pleban T, Vanoss H, et al** (1994) Mapping and introgression of a tomato yellow leaf curl virus tolerance gene, *Ty-1*. *Theor Appl Genet* **88**: 141–146